

# Re-emerging superconductivity at 48 kelvin in iron chalcogenides

Liling Sun<sup>1\*</sup>, Xiao-Jia Chen<sup>2,3\*</sup>, Jing Guo<sup>1</sup>, Peiwen Gao<sup>1</sup>, Qing-Zhen Huang<sup>4</sup>, Hangdong Wang<sup>5</sup>, Minghu Fang<sup>5</sup>, Xiaolong Chen<sup>1</sup>, Genfu Chen<sup>1</sup>, Qi Wu<sup>1</sup>, Chao Zhang<sup>1</sup>, Dachun Gu<sup>1</sup>, Xiaoli Dong<sup>1</sup>, Lin Wang<sup>6</sup>, Ke Yang<sup>7</sup>, Aiguo Li<sup>7</sup>, Xi Dai<sup>1</sup>, Ho-kwang Mao<sup>2</sup> & Zhongxian Zhao<sup>1</sup>

Pressure has an essential role in the production<sup>1</sup> and control<sup>2,3</sup> of superconductivity in iron-based superconductors. Substitution of a large cation by a smaller rare-earth ion to simulate the pressure effect has raised the superconducting transition temperature  $T_c$  to a record high of 55 K in these materials<sup>4,5</sup>. In the same way as  $T_c$  exhibits a bell-shaped curve of dependence on chemical doping, pressure-tuned  $T_c$  typically drops monotonically after passing the optimal pressure<sup>1–3</sup>. Here we report that in the superconducting iron chalcogenides, a second superconducting phase suddenly re-emerges above 11.5 GPa, after the  $T_c$  drops from the first maximum of 32 K at 1 GPa. The  $T_c$  of the re-emerging superconducting phase is considerably higher than the first maximum, reaching 48.0–48.7 K for  $\text{Tl}_{0.6}\text{Rb}_{0.4}\text{Fe}_{1.67}\text{Se}_2$ ,  $\text{K}_{0.8}\text{Fe}_{1.7}\text{Se}_2$  and  $\text{K}_{0.8}\text{Fe}_{1.78}\text{Se}_2$ .

The recent discoveries of superconductivity at 30–32 K in a new family of iron-based chalcogenide superconductors<sup>6–9</sup>  $\text{A}_{1-x}\text{Fe}_{2-y}\text{Se}_2$  (where A = K, Rb or Cs, with possible Tl substitution) bring new excitement to the field of superconductivity<sup>10</sup>. These superconductors have unusually large magnetic moments up to  $3.3\mu_B$  per Fe atom and a Fe-vacancy ordering in the Fe square lattice<sup>11</sup>. How superconductivity with such a high  $T_c$  can exist on such a strong magnetic background remains perplexing<sup>10</sup>. It has been established that superconductivity in strongly correlated electronic systems can be dictated by their crystallographic structure, electronic charge, and orbital and spin degrees of freedom, which can all be manipulated by controlling parameters such as pressure, magnetic field and chemical composition<sup>12–15</sup>. Pressure is a ‘clean’ way to tune basic electronic and structural properties without changing the chemistry. High-pressure studies are thus very useful in elucidating mechanisms of superconductivity as well as in searching for new high- $T_c$  superconducting materials.

We studied single crystals of  $\text{Tl}_{0.6}\text{Rb}_{0.4}\text{Fe}_{1.67}\text{Se}_2$ ,  $\text{K}_{0.8}\text{Fe}_{1.7}\text{Se}_2$  and  $\text{K}_{0.8}\text{Fe}_{1.78}\text{Se}_2$  grown by the Bridgman method<sup>16,17</sup>. We conducted both high-pressure resistance and susceptibility measurements to detect superconductivity *in situ* at high pressures and low temperatures. Figure 1 shows the temperature dependence of the electrical resistance at different pressures for  $\text{Tl}_{0.6}\text{Rb}_{0.4}\text{Fe}_{1.67}\text{Se}_2$  single crystals. Here we define  $T_c$  as the intersection of the tangent through the inflection point of the resistive transition with a straight-line fit of the normal state just above the transition. As can be seen,  $T_c$  starts at the maximum of 33 K at 1.6 GPa, shifts to lower temperatures at increasing pressures, and vanishes near 9 GPa in our experimental temperature range, which is 300–4 K for our high-pressure resistance measurements (Fig. 1a). At slightly higher pressures, however, an unexpected superconducting phase re-emerges with an onset  $T_c$  as high as 48.0 K at 12.4 GPa (Fig. 1b). The sample is not superconducting at pressures higher than 13.2 GPa. We repeated the measurements with new samples in three independent experiments, and the results were reproducible.

To confirm the pressure-induced changes of superconductivity in  $\text{Tl}_{0.6}\text{Rb}_{0.4}\text{Fe}_{1.67}\text{Se}_2$ , we also performed magnetic alternating-current susceptibility measurements *in situ* at high pressures (Fig. 2). The value of  $T_c$  is taken to be the onset of superconductivity defined by the intersection of a line drawn through the steep slope of the curve and the region of zero slope above the transition. The magnetic study showed that  $T_c$  decreased with increasing pressure and vanished at 9.8 GPa in the first superconducting phase SC-I (Fig. 2a). With further increasing pressure, the material enters a new superconducting phase SC-II and its transition temperature reaches 40.2 K at 12.2 GPa (Fig. 2b). The magnetic measurements yield  $T_c$  values consistent with the resistivity data within the experimental uncertainties. These results provide convincing evidence for the existence of two distinct superconducting phases in  $\text{Tl}_{0.6}\text{Rb}_{0.4}\text{Fe}_{1.67}\text{Se}_2$ .

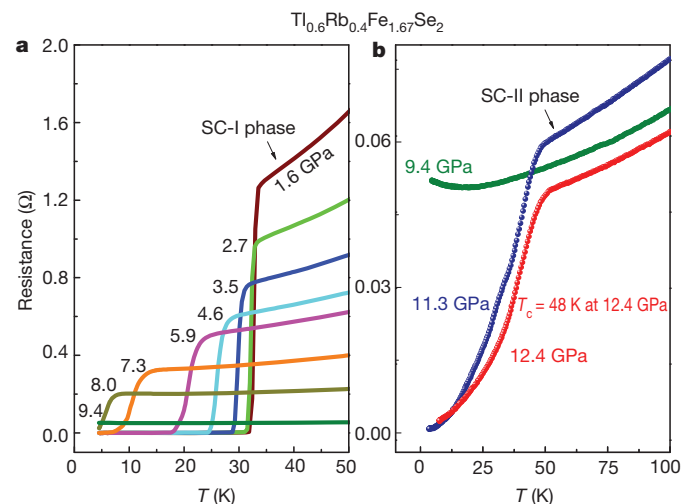


**Figure 1 | Temperature-dependence of electrical resistance for  $\text{Tl}_{0.6}\text{Rb}_{0.4}\text{Fe}_{1.67}\text{Se}_2$  at different pressures.** **a**, Resistance–temperature curves in the initial superconducting phase (SC-I) up to 9.4 GPa.  $T_c$  was observed to shift to lower temperature with increasing pressure. Superconductivity disappears at 9.4 GPa. **b**, Electrical resistance curves for the same single crystal at higher pressures. A new superconducting state re-emerges upon further compression. The pressure-induced superconducting phase (SC-II) has a  $T_c$  of 48 K, which is much higher than the maximum in SC-I. Cryogenic resistance measurements were performed in a diamond-anvil cell. Diamond anvils with 600- $\mu\text{m}$  and 300- $\mu\text{m}$  tip flats were used with sample chambers of diameter 300  $\mu\text{m}$  and 100  $\mu\text{m}$ , respectively. Four electrical leads were attached to the single-crystal sample insulated from the rhenium gasket, and loaded into the sample chamber. NaCl powders were employed as a pressure medium. The ruby fluorescence method was used to gauge pressure<sup>20</sup>.

<sup>1</sup>Institute of Physics and Beijing National Laboratory for Condensed Matter Physics, Chinese Academy of Sciences, Beijing 100190, China. <sup>2</sup>Geophysical Laboratory, Carnegie Institution of Washington, Washington DC 20015, USA. <sup>3</sup>Department of Physics, South China University of Technology, Guangzhou 510640, China. <sup>4</sup>NIST Center for Neutron Research, National Institute of Standards and Technology, Gaithersburg, Maryland 20899, USA. <sup>5</sup>Department of Physics, Zhejiang University, Hangzhou 310027, China. <sup>6</sup>HPSynC, Geophysical Laboratory, Carnegie Institution of Washington, 9700 South Cass Avenue, Argonne, Illinois 60439, USA. <sup>7</sup>Shanghai Synchrotron Radiation Facilities, Shanghai Institute of Applied Physics, Chinese Academy of Sciences, Shanghai 201204, China.

\*These authors contributed equally to this work.

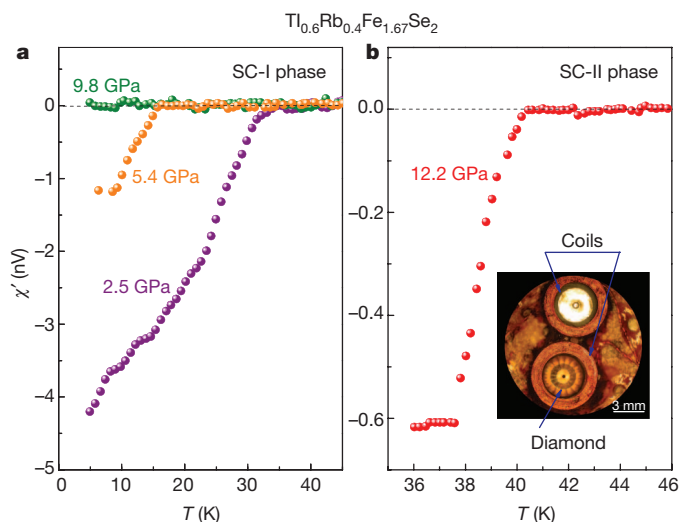


**Figure 2 | Temperature dependence of the alternating-current susceptibility for  $\text{Tl}_{0.6}\text{Rb}_{0.4}\text{Fe}_{1.67}\text{Se}_2$  at different pressures.**

**a**, Superconducting transitions in the real susceptibility component of the sample at pressures of 2.5, 5.4 and 9.8 GPa in SC-I. The superconducting transition shifts downward to lower temperature with increasing pressure. At 9.8 GPa the susceptibility component remains constant upon cooling down to 4 K, indicating that the sample is no longer superconducting. **b**, The real component of the susceptibility versus temperature for the crystal in SC-II at a pressure of 12.2 GPa. The inset shows the set-up for alternating-current susceptibility measurements in a diamond-anvil cell, with a signal coil around the diamond anvils and a compensating coil. The alternating-current susceptibilities were detected within a lock-in amplifier<sup>21</sup>. The crystals were loaded into the sample chamber, which is a hole in the centre of the nonmagnetic gaskets, with Daphne 7373 as the pressure medium.

To investigate whether the pressure-induced re-emergence of superconductivity was unique to  $\text{Tl}_{0.6}\text{Rb}_{0.4}\text{Fe}_{1.67}\text{Se}_2$  or more general among iron chalcogenides, we conducted parallel electrical resistance measurements on  $\text{K}_{0.8}\text{Fe}_{1.7}\text{Se}_2$  single crystals, and observed nearly identical behaviour (Fig. 3). The initial  $T_c$  of 32 K at 0.8–1.6 GPa decreased monotonically with increasing pressure and became undetectable at 9.2 GPa. At a slightly increased pressure, the second superconducting phase of  $\text{K}_{0.8}\text{Fe}_{1.7}\text{Se}_2$  re-emerged and reached the maximum  $T_c$  of 48.7 K

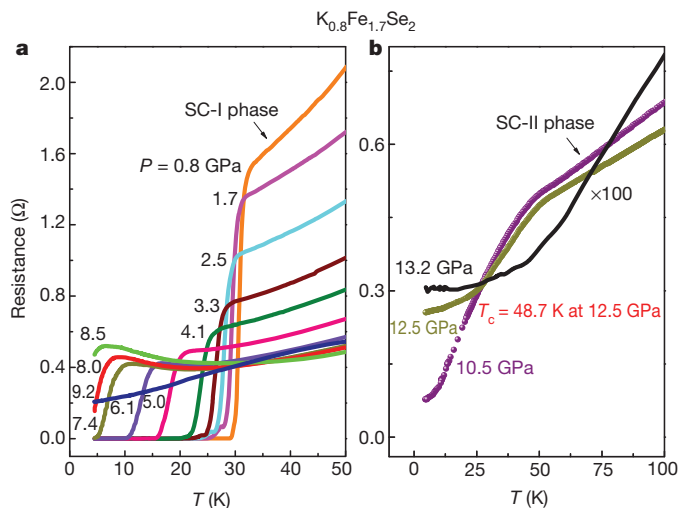


**Figure 3 | Temperature dependence of the resistance for  $\text{K}_{0.8}\text{Fe}_{1.7}\text{Se}_2$  at different pressures.** **a**, SC-I. The resistance–temperature curves showing the  $T_c$  reduction with increasing pressure and its disappearance at 9.2 GPa. **b**, SC-II. The resistance measurements reveal another superconducting phase above 10.5 GPa. The  $T_c$  reaches 48.7 K at 12.5 GPa and disappears at 13.2 GPa. The black curve has been multiplied by 100.

at 12.5 GPa. We repeated the experiment six times using six single crystals cut from different batches, and the results were reproducible. We further repeated the measurements with a slightly different composition,  $\text{K}_{0.8}\text{Fe}_{1.78}\text{Se}_2$ , and again, observed similar pressure-induced behaviour.

We summarized the pressure dependence of  $T_c$  of  $\text{Tl}_{0.6}\text{Rb}_{0.4}\text{Fe}_{1.67}\text{Se}_2$ ,  $\text{K}_{0.8}\text{Fe}_{1.7}\text{Se}_2$ , and  $\text{K}_{0.8}\text{Fe}_{1.78}\text{Se}_2$  in Fig. 4 and Supplementary Tables 1 to 4. The diagram clearly reveals two distinct superconducting regions: the initial superconducting phase SC-I and the pressure-induced superconducting phase SC-II. In the SC-I region,  $T_c$  is suppressed with applied pressure and approaches zero between 9.2 and 9.8 GPa. At higher pressures, the SC-II region appears, in which the  $T_c$  is even higher than the maximum  $T_c$  of the SC-I region. The SC-II region has a maximum  $T_c$  of 48.7 K for  $\text{K}_{0.8}\text{Fe}_{1.7}\text{Se}_2$  and 48.0 K for  $\text{Tl}_{0.6}\text{Rb}_{0.4}\text{Fe}_{1.67}\text{Se}_2$ , higher than previously observed in chalco-genide superconductors. The SC-II region appears in a narrow pressure range. Unlike the usual parabolic pressure-tuning curve of  $T_c$ , the high  $T_c$  in SC-II appears abruptly above 9.8 GPa and disappears equally abruptly above 13.2 GPa. Intermediate  $T_c < 38$  K is not observed even with small pressure increment steps of 0.1 GPa. A similar re-emergence of superconductivity has been observed in some other strongly correlated electronic systems, such as heavy-fermion<sup>12</sup> and organic systems<sup>18</sup>.

Our preliminary high-pressure polycrystalline X-ray diffraction results of the two iron chalcogenides  $\text{K}_{0.8}\text{Fe}_{1.7}\text{Se}_2$  and  $\text{K}_{0.8}\text{Fe}_{1.78}\text{Se}_2$  confirm that, to the first degree, the basic tetragonal crystal structure persists throughout the pressure range studied (Supplementary Information). Therefore, the disappearance of  $T_c$  in SC-I, the re-emergence of higher  $T_c$  in SC-II, and the final non-superconducting region reflect detailed structural variances within the basic tetragonal unit cell, which await future in-depth investigation with advanced diagnostic probes. For instance, the possible change in magnetic-ordering structures would require high-pressure neutron diffraction, and the possible superlattice and Fe vacancy ordering would require high-pressure single-crystal X-ray structural investigations.

The pressure dependence of  $T_c$  in the SC-I region is expected but its mechanism is still much debated. Quantum criticalities are thought to affect superconductivity for strongly correlated electronic systems<sup>19</sup>. A characteristic feature of the new iron chalcogenide superconductors is

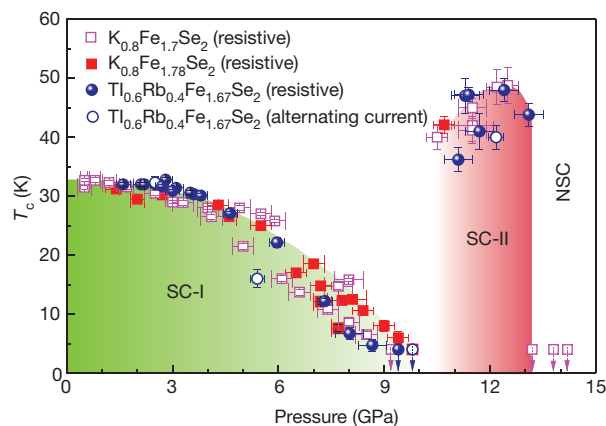


**Figure 4 | Pressure dependence of the  $T_c$  for  $\text{Tl}_{0.6}\text{Rb}_{0.4}\text{Fe}_{1.67}\text{Se}_2$ ,  $\text{K}_{0.8}\text{Fe}_{1.7}\text{Se}_2$  and  $\text{K}_{0.8}\text{Fe}_{1.78}\text{Se}_2$ .** The symbols represent the pressure–temperature conditions for which  $T_c$  values were observed from the resistive and alternating-current susceptibility measurements; symbols with downward arrows represent the absence of superconductivity to the lowest temperature (4 K). All  $\text{Tl}_{0.6}\text{Rb}_{0.4}\text{Fe}_{1.67}\text{Se}_2$ ,  $\text{K}_{0.8}\text{Fe}_{1.7}\text{Se}_2$  and  $\text{K}_{0.8}\text{Fe}_{1.78}\text{Se}_2$  samples show two superconducting regions (SC-I and SC-II) separated by a critical pressure at around 10 GPa. NSC, the non-superconducting region above 13.2 GPa. The maximum  $T_c$  is found to be 48.7 K in  $\text{K}_{0.8}\text{Fe}_{1.7}\text{Se}_2$  at a pressure of 12.5 GPa. At higher pressures above 13.2 GPa, the samples are non-superconducting. Error bars are one standard deviation.

the existence of Fe-vacancies in the Fe-square lattice, ordered by a  $\sqrt{5} \times \sqrt{5}$  superstructure<sup>11</sup>. It remains unclear whether pressure could destroy the vacancy ordering at a critical value and drive the materials into a disordered lattice. Detailed structural studies of these superconducting behaviours in the iron chalcogenide superconductors are currently being conducted. Their magnetic properties at high pressures should help us to understand the interplay of magnetism and superconductivity in these iron chalcogenides.

This observation of the SC-II region with the re-emerging higher  $T_c$  is unexpected. It will certainly stimulate a great deal of future experimental and theoretical studies to clarify whether the observed re-emergence of superconductivity in iron chalcogenides is associated with the quantum critical transition, magnetism, superstructure, vacancy ordering or spin fluctuation.

Received 21 October; accepted 19 December 2011.

Published online 22 February 2012.

- Torikachvili, M. S., Bud'ko, S. L., Ni, N. & Canfield, P. C. Pressure induced superconductivity in  $\text{CaFe}_2\text{As}_2$ . *Phys. Rev. Lett.* **101**, 057006 (2008).
- Takahashi, H. *et al.* Superconductivity at 43 K in an iron-based layered compound  $\text{LaO}_{1-x}\text{F}_x\text{FeAs}$ . *Nature* **453**, 376–378 (2008).
- Medvedev, S. *et al.* Electronic and magnetic phase diagram of  $\beta\text{-Fe}_{1.01}\text{Se}$  with superconductivity at 36.7 K under pressure. *Nature Mater.* **8**, 630–633 (2009).
- Chen, X. H. *et al.* Superconductivity at 43 K in  $\text{SmFeAsO}_{1-x}\text{F}_x$ . *Nature* **453**, 761–762 (2008).
- Ren, Z. A. *et al.* Superconductivity at 55 K in iron-based F-doped layered quaternary compound  $\text{Sm}[\text{O}_{1-x}\text{F}_x]\text{FeAs}$ . *Chin. Phys. Lett.* **25**, 2215–2216 (2008).
- Guo, J. G. *et al.* Superconductivity in the iron selenide  $\text{K}_x\text{Fe}_2\text{Se}_2$  ( $0 < x < 1.0$ ). *Phys. Rev. B* **82**, 180520(R) (2010).
- Krzton-Maziopa, A. *et al.* Synthesis and crystal growth of  $\text{Cs}_{0.8}(\text{FeSe}_{0.98})_2$ : a new iron-based superconductor with  $T_c = 27$  K. *J. Phys. Condens. Matter* **23**, 052203 (2011).
- Wang, A. F. *et al.* Superconductivity at 32 K in single-crystalline  $\text{Rb}_x\text{Fe}_{2-y}\text{Se}_2$ . *Phys. Rev. B* **83**, 060512(R) (2011).
- Fang, M. H. *et al.* Fe-based superconductivity with  $T_c = 31$  K bordering an antiferromagnetic insulator in  $(\text{Ti},\text{K})\text{Fe}_x\text{Se}_2$ . *Europhys. Lett.* **94**, 27009 (2011).
- Mazin, I. Iron superconductivity weathers another storm. *Physics* **4**, 26 (2011).
- Bao, W. *et al.* A novel large moment antiferromagnetic order in  $\text{K}_{0.8}\text{Fe}_{1.6}\text{Se}_2$  superconductor. *Chin. Phys. Lett.* **28**, 086104 (2011).
- Yuan, H. Q. *et al.* Observation of two distinct superconducting phases in  $\text{CeCu}_2\text{Si}_2$ . *Science* **302**, 2104–2107 (2003).
- Chen, X. J. *et al.* Enhancement of superconductivity by pressure-driven competition in electronic order. *Nature* **466**, 950–953 (2010).
- Uji, S. *et al.* Magnetic-field-induced superconductivity in a two-dimensional organic conductor. *Nature* **410**, 908–910 (2001).
- Jin, K., Butch, N. P., Kirshenbaum, K. & Greene, R. L. Link between spin fluctuations and electron pairing in copper oxide superconductors. *Nature* **476**, 73–75 (2011).
- Wang, D. M., He, J. B., Xia, T.-L. & Chen, G. F. The effect of varying Fe-content on transport properties of K intercalated iron selenide  $\text{K}_x\text{Fe}_{2-y}\text{Se}_2$ . *Phys. Rev. B* **83**, 132502 (2011).
- Wang, H. D. *et al.* Superconductivity at 32 K and anisotropy in  $\text{Tl}_{0.58}\text{Rb}_{0.42}\text{Fe}_{1.72}\text{Se}_2$  crystals. *Europhys. Lett.* **93**, 47004 (2011).
- Okuhata, T. *et al.* High-pressure studies of doped-type organic superconductors. *J. Phys. Soc. Jpn* **76** (Suppl. A) 188–189 (2007).
- Si, Q. M. & Steglich, F. Heavy fermions and quantum phase transitions. *Science* **329**, 1161–1166 (2010).
- Mao, H. K., Xu, J. & Bell, P. M. Calibration of the ruby pressure gauge to 800 Kbar under quasi-hydrostatic conditions. *J. Geophys. Res.* **91**, 4673–4676 (1986).
- Debessai, M., Matsuoka, T., Hamlin, J. J. & Schilling, J. S. Pressure-induced superconducting state of europium metal at low temperatures. *Phys. Rev. Lett.* **102**, 197002 (2009).

Supplementary Information is linked to the online version of the paper at [www.nature.com/nature](http://www.nature.com/nature).

**Acknowledgements** We thank I. I. Mazin, W. Bao, and T. Xiang for discussions and J. S. Schilling for the help with the alternating-current susceptibility technique. This work in China was supported by the NSCF, 973 projects, and Chinese Academy of Sciences. This work in the USA was supported as part of the EFree, an Energy Frontier Research Center funded by the US Department of Energy, Office of Science, Office of Basic Energy Sciences (DOE-BES). The High Pressure Collaborative Access Team (HPCAT) is supported by CIW, CDAC, UNLV and LLNL through funding from the DOE-NNSA, the DOE-BES and the NSF. The Advanced Photon Source (APS) is supported by the DOE-BES.

**Author Contributions** L.S., X.-J.C., H.M. and Z.Z. designed the project; X.-J.C., L.S., H.M., Q.W. and Z.Z. wrote the paper; P.G., J.G., C.Z. and L.S. performed the resistance and magnetic susceptibility measurements; X.-J.C., L.W., J.G., P.G., L.S., K.Y. and A.L. performed synchrotron X-ray diffraction measurements; and M.F., X.C. and G.C. synthesized the single crystals. All the authors analysed the data and discussed the results. All the authors read and commented on the manuscript.

**Author Information** Reprints and permissions information is available at [www.nature.com/reprints](http://www.nature.com/reprints). The authors declare no competing financial interests. Readers are welcome to comment on the online version of this article at [www.nature.com/nature](http://www.nature.com/nature). Correspondence and requests for materials should be addressed to Z.Z. ([zhxzhao@iphy.ac.cn](mailto:zhxzhao@iphy.ac.cn)) or H.M. ([hmao@gl.ciw.edu](mailto:hmao@gl.ciw.edu)).